Open Access

SCHOLARENA

Journal of Food Technology and Food Chemistry

RESEARCH ARTICLE

ISSN: 2641-8118

Improving Functional Properties of Soy Protein Isolates through Ultrasound: Physicochemical, Emulsifying, and Gel-like Characteristics

Nebahat Taş[1], Emine Erçelebi[1,*] and Hatice Pekmez[2,*]

[1]*Gaziantep University, Faculty of Engineering, Department of Food Engineering, Gaziantep, 27310 Gaziantep, Türkey*

[2]*Gaziantep University, Faculty of Tourism, Department of Gastronomy and Culinary Arts, Gaziantep, 27310 Gaziantep, Türkey*

[*]**Corresponding Authors:** Emine Erçelebi, 1Gaziantep University, Faculty of Engineering, Department of Food Engineering, Gaziantep, 27310 Gaziantep, Türkey, E-mail: alben@gantep.edu.tr

Hatice Pekmez, Gaziantep University, Faculty of Tourism, Department of Gastronomy and Culinary Arts, Gaziantep, 27310 Gaziantep, Türkey, E-mail: pekmez@gantep.edu.tr

Citation: Nebahat Taş, Emine Erçelebi, Hatice Pekmez (2025) Improving Functional Properties of Soy Protein Isolates through Ultrasound: Physicochemical, Emulsifying, and Gel-like Characteristics, J Food Tech nol Food Chem 7: 103

Abstract

This study comprehensively investigated the impact of ultrasound treatment, thermal processing, and pH modulation on the physicochemical, emulsifying, and gel-forming properties of soy protein isolate (SPI), aiming to optimize its functionality for advanced food applications. SPI solutions were sonicated at amplitudes of 5, 10, and 15, followed by evaluations of droplet size, emulsifying activity index (EAI), and emulsifying stability index (ESI). Ultrasound significantly enhanced EAI and ESI in a dose-dependent manner, with the most pronounced improvements at 15 amplitude, driven by partial protein unfolding, aggregate disruption, and increased surface hydrophobicity. Complementary heat treatments (60–80 °C) and pH adjustments (5, 7, 9) further improved emulsion stability, particularly under alkaline conditions and elevated temperatures, which promoted solubility and interfacial adsorption. In the second phase, gel-like emulsions were developed via cold-set and heat-set methods using $CaSO_4$. Only formulations containing 6–7% (w/v) SPI formed stable viscoelastic networks, with heat-set gels showing superior water- and fat-holding capacities, smaller droplet sizes, and more compact microstructures. These enhancements were attributed to thermally induced protein aggregation and ultrasound-enhanced interfacial organization. Microscopic and rheological analyses confirmed that heat-treated, ultrasound-preconditioned SPI formed denser and more uniform matrices, ideal for encapsulating lipophilic compounds. Overall, the combined application of ultrasound, heat, and pH control effectively tailored the interfacial and structural properties of SPI-based systems. These findings offer promising avenues for developing clean-label, plant-based emulsions and gel-like matrices with enhanced stability, texture, and functionality, suitable for nutraceutical delivery and health-oriented food formulations.

Keywords: Soy Protein; Ultrasound; Plant-based Emulsion; Gel-like Emulsion; Functional Food Systems

Introduction

Soy protein has become a focal point in food science and nutrition research, largely due to its excellent nutritional profile, particularly its high protein content of 38–40%, and its wide applicability in various food systems [1]. It is not only a sustainable alternative to animal proteins but also a functional ingredient widely used in emulsified meat products, baked goods, and plant-based meat analogues [2, 3]. Recent studies also highlight its low allergenicity compared to other legumes and its beneficial effects on gut microbiota, which further support its integration into functional foods [4, 5]. With growing public interest in health and wellness, food products enriched with bioactive compounds such as antioxidants, antimicrobials, and phytochemicals are increasingly favored over traditional pharmaceutical approaches [6, 7]. Soy proteins have also been identified as promising carriers for microencapsulation of bioactives, improving their bioavailability and stability in gastrointestinal environments [8].

Proteins play a dual role in food systems: while they serve as essential nutrients, their structural features also grant them unique functional properties. These properties, such as solubility, emulsification, gelation, and water-binding capacity, are closely linked to the amino acid sequence, molecular conformation, and interactions within the food matrix [9, 10]. Both animal-based and plant-based proteins are utilized for their technological functionality, but plant proteins, especially soy, are gaining attention due to their environmental and nutritional advantages [11, 12].

Among plant-derived proteins, soy protein isolate (SPI) is particularly valued for its functionality and economic viability. Its major protein fractions, β-conglycinin (7S) and glycinin (11S), enable it to perform key roles in emulsion formation and gelation. These capabilities are linked to its surface hydrophobicity and the ability to form various molecular interactions, including hydrogen bonding and disulfide cross-linking [13-16]. Advanced characterization techniques such as confocal laser scanning microscopy (CLSM) and low-field NMR have recently been employed to elucidate the gelation behavior of SPI under different conditions, offering deeper insight into its structural dynamics [17, 18].

Recently, one of the most promising developments in food protein science has been the creation of gel-like emulsions—semi-solid, viscoelastic systems that can encapsulate lipophilic nutrients such as polyunsaturated fatty acids and carotenoids. These emulsions not only exhibit improved physical stability (resisting phase separation, creaming, and coalescence) but also offer potential for targeted and controlled delivery of sensitive bioactives [19-22]. The incorporation of natural emulsifiers and stabilizers alongside soy proteins, such as polysaccharides and dietary fibers, has further enhanced the rheological behavior and oxidative stability of these emulsions [23, 24].

To enhance the performance of such systems, high-intensity ultrasound (HIU) has emerged as a novel processing technology. Operating typically between 20–100 kHz, HIU generates acoustic cavitation, which leads to physical changes in protein conformation without compromising their nutritional integrity. This process disrupts aggregates, increases solubility, and improves interfacial activity without denaturing the protein [25, 26]. Research has shown that HIU enhances the surface hydrophobicity and sulfhydryl content of SPI, contributing to stronger gels with improved water-holding capacity [27, 14, 28]. Moreover, emerging findings suggest that HIU can be synergistically combined with other green technologies, such as pulsed electric fields or ohmic heating, to optimize soy protein functionality [29, 30].

Despite these advances, there is still limited understanding of how ultrasound interacts with other variables such as heat, pH, and protein concentration within gel-like emulsion systems. Most existing studies have centered on conventional heat-induced or enzymatically formed gels, often overlooking the complex synergies that arise under combined treatments [31, 21, 28]. Comprehensive multivariate models and real-time rheokinetics are now being explored to predict and control gelation behavior in such complex systems, pointing toward precision formulation in food design [32].

Therefore, this study aims to investigate how ultrasound treatment influences the physicochemical, emulsifying, and gel-forming properties of soy protein isolate. The research is structured in two phases. In the first phase, emulsions were prepared with SPI at different concentrations and exposed to various ultrasound amplitudes under controlled pH and temperature conditions to examine their stability and functionality. In the second phase, both heat-set and cold-set gel-like emulsions were created using varying protein and oil levels, and water-holding capacity, and microstructure were evaluated. The findings contribute to a better understanding of ultrasound-mediated protein structuring and provide valuable insight for the development of next-generation functional foods and nutraceutical delivery systems.

Materials and Methods

Materials

Soy protein isolate (SPI), sodium dodecyl sulfate (SDS), and calcium sulfate were purchased from Sigma-Aldrich Chemicals Co. (St. Louis, MO, USA). Commercial-grade soybean oil was sourced from a local market and used without further purification. Distilled water was used for all solution preparations and analytical procedures. pH adjustments were performed using either 0.1 N sodium hydroxide (NaOH ≥97%, Merck Chemicals Co., Darmstadt, Germany) or 0.1 N hydrochloric acid (HCl, 37.0%, Merck Chemicals Co.). All other reagents were of analytical grade and obtained from Sigma-Aldrich.

Methods

Preparation of Soy Protein Isolate Solutions

Soy Protein Isolate (SPI) solutions were prepared at concentrations of 1% and 3% (w/v) by dissolving the appropriate amount of SPI powder in 10 mL of distilled water. The mixtures were stirred at room temperature using a magnetic stirrer (Model MS300HD, MTops Co. Ltd., Korea) for 15 minutes to ensure complete dissolution.

Ultrasound Treatment

Ultrasound treatment was carried out by following the method of Zhang et al. (2016), with slight modifications. A Soniprep 150 ultrasonic disintegrator (MSE, Ramco Co. Ltd., Lincolnshire, UK) equipped with a 0.636 cm diameter titanium probe was used. The SPI solutions were treated at amplitudes of 5, 10, and 15 for 1 minute.

Emulsion Preparation

Ultrasound-treated SPI solutions (1% and 3%, w/v) were used to prepare emulsions by adding 10% (v/v) soybean oil. The mixtures were homogenized at 10,000 rpm for 2 minutes using a high-speed homogenizer (IKA T-18 Digital ULTRA TURRAX, Sigma-Aldrich Co., St. Louis, MO) equipped with an S18N-10G stainless steel dispersing element. The emulsions were subsequently analyzed for emulsifying activity index (EAI), emulsifying stability index (ESI), creaming behavior, and microscopic droplet size.

Heat Treatment on Emulsions

To evaluate the impact of thermal treatment, SPI solutions (1% and 3%, w/v) were heated to 60, 70, and 80°C in a water bath for 2 minutes, based on the method of Gu et al. [33] with modifications. The heated solutions were then rapidly cooled in an ice bath (Model SWB15D, Camlab, UK). After cooling, they were sonicated at an amplitude of 15 for 1 minute. Subsequently, 10% (v/v) soybean oil was added, and the mixtures were homogenized at 10,000 rpm for 2 minutes to form emulsions.

pH Adjustment of Emulsions

The effect of pH on emulsion properties was examined by adjusting the pH of SPI solutions (1% and 3%, w/v) to 5, 7, and 9 using 0.1 N NaOH or 0.1 N HCl, according to the method of Li et al. (2012) [34]. pH measurements were conducted using a microprocessor pH meter (Model 211, Hanna Instruments Co., Woonsocket, USA), calibrated with standard buffer solutions at pH 4.0 and 9.0. The pH-adjusted solutions were sonicated at an amplitude of 15 for 1 minute. Soybean oil (10%, v/v) was then added to each solution, followed by homogenization at 10,000 rpm for 2 minutes to form emulsions.

Emulsifying Activity and Stability Index of Emulsions

The emulsifying activity index (EAI) of the protein-stabilized emulsions was determined according to the method of Pearce and Kinsella (1978) [35], with minor modifications. Emulsions containing 1% and 3% (w/v) soy protein isolate were prepared and subjected to ultrasound treatment at amplitudes of 5, 10, and 15 for 1 minute. Subsequently, 10% (v/v) soybean oil was added, and the mixtures were homogenized at 10,000 rpm for 2 minutes.

To evaluate the EAI, 50 μL of freshly prepared emulsion was immediately diluted in 0.2 M SDS solution. Then, 1 mL of the diluted emulsion was transferred to a 1 cm path length cuvette, and the absorbance was measuerd at 500 nm using a spectrophotometer (Pharmacia Biotech Novaspec II, Cambridge, UK). Absorbance readings were recorded at 0 minutes and again after 10 minutes to assess emulsion stability.

The turbidity (T) was calculated using the equation:

where A is the absorbance and L is the cuvette path length (cm).

The emulsifying activity index (EAI, m^2/g) was calculated as:

where F is dilution factor, ⊠ is the volumetric fraction of oil and C is the concentration of protein (g/mL) in the aqueous phase [36].

The emulsifying stability index (ESI, min) was calculated using the following equation:

where A_0 and A_{10} represent the absorbance values measured at 0 and 10 minutes, respectively [37].

Creaming Stability of Emulsions

Creaming stability was evaluated according to the method described by Wang et al. [37]. Emulsions containing 1% and 3% (w/v) soy protein isolate were prepared in 10 mL volumes and left undisturbed at room temperature for 10 hours. The extent of phase separation was visually monitored, and creaming was quantified as the percentage of the serum layer volume relative to the total emulsion volume using the following equation:

$$Creaming(\%) = \left(\frac{\text{Volume of the serum layer}}{\text{Volume of the emulsion}}\right) \times 100$$

Viscosity of Emulsion

The apparent viscosity of emulsions was measured using a DV2T rotational viscometer (Brookfield Rheometer) at a fixed shear rate of 40 s^{-1}. A 0.5 mL aliquot of freshly prepared emulsion was introduced into the viscometer sample holder using a pipette, and measurements were taken at room temperature.

Optical Microscopy

The microstructure of the emulsions was examined using polarized light microscopy, following the method described by Erçelebi et al. [35]. A single drop of freshly prepared emulsion was placed onto a microscope slide, covered with a coverslip, and observed under an Olympus BX51 microscope (Olympus, Tokyo, Japan) equipped with a Pixera PVC100C video camera (USA). Images were captured using a 10× magnification objective. The droplet size distribution was analyzed using the BAB software integrated with the microscope system. Diameters of 100 individual droplets were measured, and the average value was recorded.

Preparation of Gel-Like Emulsions

Gel-like emulsions were prepared using the method of Hu et al. (2013), with slight modifications. SPI solutions were prepared at concentrations of 1%, 3%, 5%, 6%, 7%, 8%, and 10% (w/v) in distilled water. Each solution was sonicated at an amplitude of 15 for 1 minute. Soybean oil was added at either 10% or 30% (v/v), and the mixtures were homogenized at 10,000 rpm for 2 minutes.

For cold-set gelation, 0.2 mL of 0.2 M $CaSO_4$ solution was added to the emulsions and mixed thoroughly. The samples were then stored at 4°C for 24 hours to allow gel-like structures to develop. For heat-set gelation, the same volume of $CaSO_4$ solution was added, after which the emulsions were heated at 95°C in a water bath for 20 minutes. Following thermal treatment, the emulsions were rapidly cooled in an ice bath and subsequently stored at 4°C for 24 hours to allow gel formation.

Water Holding Capacity of Gel-like Emulsions

The water-holding capacity (WHC) of the gel-like emulsions was determined by following the method of Yang et al. [38], with slight modifications. A 10 g sample of each gel-like emulsion was transferred into 50 mL centrifuge tubes and centrifuged at 8000×g for 30 minutes at 4°C. The released water was separated using dry filter paper.

The weight of each tube was recorded before and after centrifugation to calculate the amount of water released. WHC was expressed as the percentage of retained water relative to the total water content in the emulsion and calculated using the following formula:

$$WHC(\%) = \frac{W_t - W_f}{W_t} \times 100$$

where W_t represents the total weight of water added to the emulsion (g), and W_f is the weight of water released after centrifugation (g).

Fat Holding Capacity of Gel-Like Emulsions

The fat-holding capacity (FHC) of the gel-like emulsions was assessed based on the method of Gu et al. (2009) [33], with slight modifications. A total of 20 mL of SPI-based gel-like emulsions was prepared and centrifuged at 10,000×g for 30 minutes. The resulting precipitate was then mixed with 10 mL of 5% (w/v) potassium hydroxide (KOH) and homogenized using an Ultra--Turrax homogenizer for 1 minute. The samples were stored for 48 hours, after which the separated fat layer at the top was visually quantified.

FHC was calculated using the following equation:

$$\text{FHC } (\%) = \frac{F_a}{F_t} \times 100$$

where F_t is the total volume of oil (mL) initially added to the emulsion, and F_a is the volume of oil retained within the gel matrix after separation.

Statistical Analysis

All experiments were conducted in triplicate. The data were analyzed using one-way analysis of variance (ANOVA) to determine statistically significant differences among the means. Post hoc comparisons were performed using Tukey's multiple range test at a significance level of $p<0.05$. Statistical analysis was conducted using SPSS software (Version 25.0, IBM Corp., Armonk, NY, USA). Graphical representations of the results were generated using Microsoft Office software.

Results and Discussion

Effect of Ultrasound Treatment

Emulsifying Activity and Stability Index of Ultrasound-Treated Emulsions

The emulsifying activity index (EAI) reflects a protein's ability to adsorb at the oil–water interface, indicating the interfacial area stabilized per gram of protein [37]. In the present study, emulsions were prepared using soy protein isolate (SPI) at concentrations of 1% and 3% (w/v) and treated with ultrasound at amplitudes of 5, 10, and 15. As depicted in Figures 3.1a, the EAI increased significantly with both higher protein concentration and ultrasound amplitude ($p<0.05$). Specifically, at 1% SPI, EAI values were 667.87, 870.54, and 1036.35 m^2/g for 5, 10, and 15 amplitude, respectively. In contrast, emulsions containing 3% SPI exhibited markedly higher EAI values of 1137.68, 1501.56, and 1782.52 m^2/g under the same amplitude conditions. These results highlight the combined effect of higher protein concentration and ultrasound intensity in enhancing emulsifying performance through improved interfacial activity. This enhancement can be attributed to the greater availability of surface-active protein at higher concentrations, as well as the structural modifications induced by ultrasound, such as partial unfolding, exposure of hydrophobic groups, and reduction of protein aggregate size [38, 39]. These structural changes increase protein–oil interactions, decrease interfacial tension, reduce droplet size and enhance droplet coverage during homogenization [40, 41]. Additionally, ultrasound increases the accessibility of buried functional groups, which can further improve emulsification efficiency [26]. Recent proteomic analyses have confirmed that sonication induces conformational changes in SPI, particularly increasing β-sheet to random coil transitions, which is associated with enhanced emulsifying capacity [42].

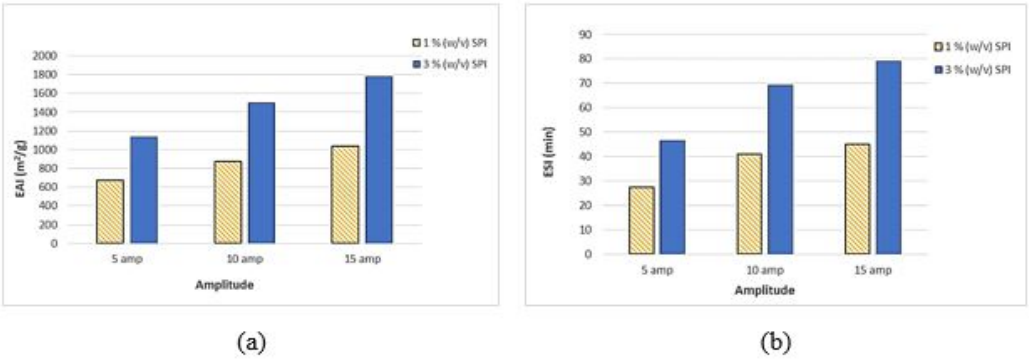

Figure 3.1: Emulsifying properties of SPI-stabilized emulsions at different ultrasound amplitudes: (a) EAI, (b) ESI

Creaming Stability of Ultrasound-Treated Emulsions

Creaming, defined as the upward migration of oil droplets due to density differences between the dispersed and continuous

phases, is a key indicator of emulsion instability. In this study, creaming behavior was monitored over a 10-hour period, as shown in Figure 3.2. At the lowest ultrasound amplitude (5 amp), creaming was most pronounced, reaching 28.6% and 27.0% for emulsions containing 1% and 3% (w/v) SPI, respectively. As ultrasound amplitude increased, creaming values decreased significantly ($p<0.05$), reflecting enhanced emulsion stability. Notably, at 15 amp and 3% SPI, creaming was minimized to 19.9%, demonstrating the beneficial effects of both higher ultrasound intensity and protein concentration on emulsion stability. This improvement is likely due to enhanced droplet size reduction, improvement in interfacial adsorption of proteins and change in viscosity of emulsions due to increased protein content which all together reduce droplet migration and phase separation [38, 14]. The improved stability is attributed to ultrasound-induced reduction in droplet size and the formation of more homogeneous and compact interfacial layers [40]. Studies using multiple light scattering (Turbiscan) techniques confirmed that sonicated SPI emulsions exhibit lower instability indices and delayed creaming onset compared to untreated samples [45].

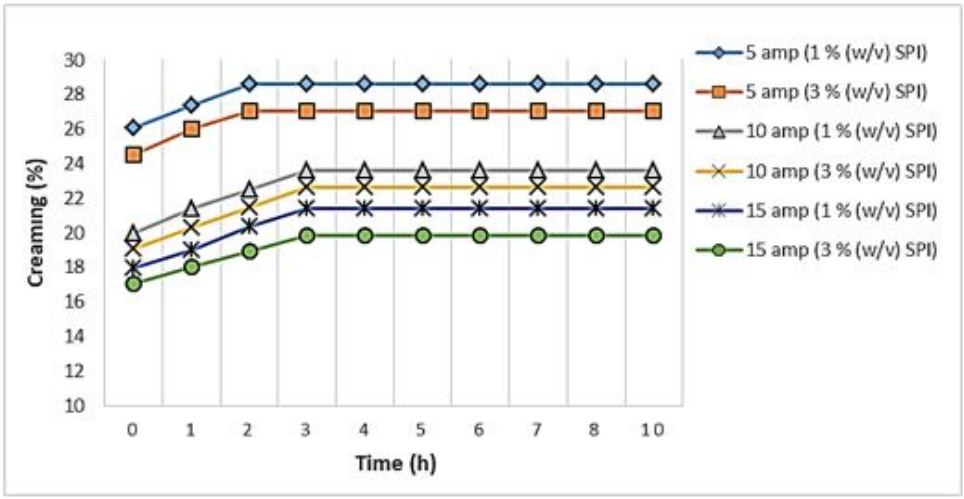

Figure 3.2. Creaming behavior of SPI-stabilized emulsions at different ultrasound amplitudes

Microscopic Observation of Ultrasound-Treated Emulsions

Microscopic observations (Figure 3.3) and droplet size measurements (Table 3.1) further confirmed the impact of ultrasound treatment on emulsion structure. At a lower protein concentration (1% w/v SPI) and low ultrasound amplitude (5 amp), emulsions exhibited large and irregular oil droplets with an average size of 12.05 μm. In contrast, increasing both the protein concentration to 3% and the ultrasound amplitude to 15 amp resulted in significantly smaller and more uniform droplets ($p<0.05$), with an average size of 6.57 μm. These findings highlight the effectiveness of ultrasound in enhancing emulsion homogeneity by promoting droplet disruption and reducing average droplet size. Ultrasound facilitates the breakdown of protein aggregates and increases exposure of hydrophobic domains, promoting efficient interfacial adsorption and uniform droplet dispersion [46, 47]. Recent SEM and CLSM studies have demonstrated that HIU-treated emulsions exhibit denser and more continuous interfacial protein films, which correlates with reduced droplet coalescence and improved physical stability [48].

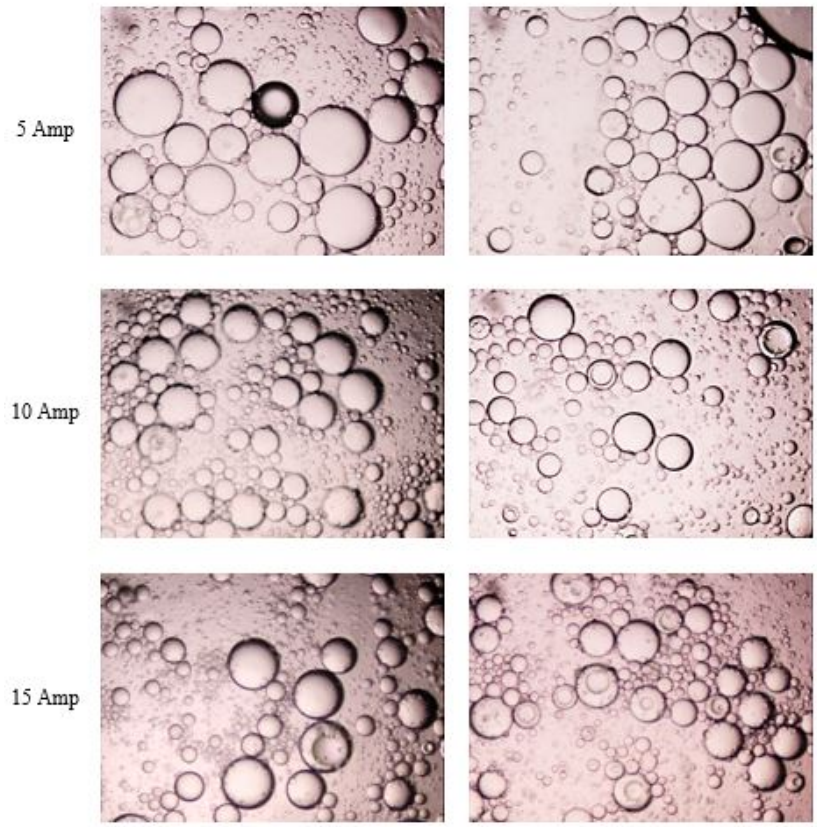

Figure 3.3: Microstructure of SPI-stabilized emulsions with varying protein concentrations at different ultrasound amplitudes: (a) 1% (w/v) SPI, (b) 3% (w/v) SPI

Viscosity of Ultrasound-Treated Emulsions

Viscosity is a critical physicochemical parameter that influences both the stability and sensory attributes of emulsions. As illustrated in Figure 3.4, viscosity values significantly increased ($p<0.05$) with rising ultrasound amplitude and protein concentration. For emulsions containing 1% (w/v) SPI, viscosity increased from 2.72 cP at 5 amp to 4.38 cP at 15 amp. In the case of 3% SPI, the viscosity rose more markedly, from 3.34 cP to 9.74 cP across the same amplitude range. These increases are likely associated with the formation of smaller droplet sizes and enhanced inter-droplet interactions, both of which contribute to a more structured and viscous emulsion system. Increased protein unfolding and droplet surface coverage after sonication contribute to a denser continuous phase and higher viscosity [41]. This behavior is favorable for emulsion stability and texture, particularly in functional food applications. Rheological modeling (e.g., Herschel–Bulkley analysis) has confirmed that ultrasound induces pseudoplastic behavior with higher yield stress and consistency coefficients, indicating structural reinforcement of emulsified systems [49].

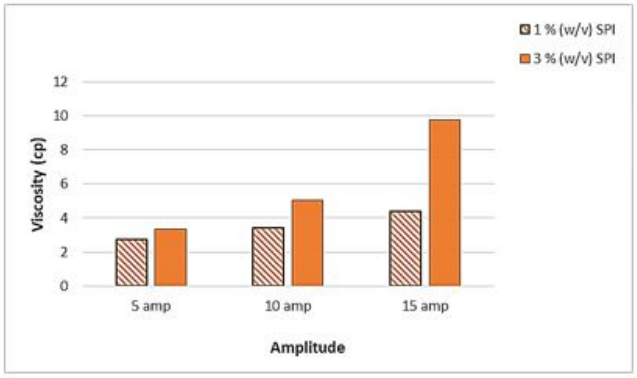

Figure 3.4: Viscosity of SPI-stabilized emulsions at different ultrasound amplitudes

Effect of Heat Treatment on Emulsions

Emulsifying Activity and Stability Index of Heat-Treated Emulsions

The EAI of SPI-stabilized emulsions subjected to thermal treatment at 60, 70, and 80 °C is presented in Figures 3.5a. At each temperature, emulsions prepared with 3% (w/v) SPI consistently exhibited significantly higher EAI values than those formulated with 1% SPI ($p<0.05$), indicating a positive correlation between protein concentration and emulsification efficiency under heat treatment. For emulsions containing 1% SPI, EAI values were 884.35, 1063.99, and 1202.17 m^2/g at 60, 70, and 80 °C, respectively. In comparison, emulsions with 3% SPI showed notably enhanced EAI values of 1317.32, 1561.43, and 1625.92 m^2/g across the same temperature range. These results suggest that elevated temperatures, in conjunction with higher protein concentrations, promote improved interfacial adsorption and unfolding of protein molecules, thereby enhancing the emulsifying properties of SPI. The increase in EAI can be attributed to elevated thermal energy enhancing protein flexibility, allowing better interfacial adsorption and more efficient droplet stabilization [14, 38]. Furthermore, heat treatment can promote the exposure of hydrophobic groups and improve protein solubility, contributing to increased emulsifying capacity [50]. Recent studies using Fourier-transform infrared spectroscopy (FTIR) and circular dichroism have shown that thermal unfolding leads to a decrease in α-helix content and an increase in β-sheet structures, which enhances emulsifying behavior by improving interfacial anchoring of SPI molecules [51].

Table 3.1 Effect of ultrasound, heating, and pH on droplet size of SPI-stabilized emulsions at different protein concentrations

Treatment	Condition	Droplet Size (μm) *SPI concentration 1 % (w/v) 3 % (w/v)*	
Ultrasound	5 amp	12.05^{aA}	9.28^{aB}
	10 amp	8.48^{bA}	7.88^{bB}
	15 amp	7.72^{cA}	6.57^{cB}
Temperature	60°C	9.84^{aA}	8.93^{aB}
	70°C	6.70^{bA}	5.88^{bB}
	80°C	4.54^{cA}	4.17^{cB}
pH	pH 5	10.91^{aA}	9.78^{aB}
	pH 7	9.99^{bA}	6.82^{bB}
	pH 9	8.93^{cA}	6.17^{cB}

Different lowercase superscript letters within the same column and uppercase letters within the same row indicate statistically significant differences at the p<0.05 level for each treatment.

Table 3.2: Droplet size of gel-like emulsions at different oil and protein concentrations

Set method	Droplet Size (µm)		
	Oil concentration	*SPI concentration*	
	(v/v)	*6 % (w/v)*	*7 % (w/v)*
Cold-set	10%	7.97^{aA}	6.83^{aB}
	30%	7.11^{bA}	5.98^{bB}
Heat-set	10%	6.92^{aA}	5.64^{aB}
	30%	6.15^{bA}	4.67^{bB}

Different lowercase superscript letters within the same column and uppercase letters within the same row indicate statistically significant differences at the p<0.05 level for each set.

Similarly, the ESI, which indicates the ability of emulsions to resist destabilization over time, significantly increased (p<0.05) with rising temperature and protein concentration (Figure 3.5b). At 60 °C, ESI values were 45 minutes for emulsions containing 1% (w/v) SPI and 76 minutes for those with 3% SPI. With further heating to 70 °C, these values increased to 55 and 89 minutes, respectively, and reached their maximum at 80 °C, with ESI values of 65 minutes for 1% SPI and 101 minutes for 3% SPI. The results demonstrate that both thermal treatment and higher protein concentration contribute positively to emulsion stability by enhancing interfacial interactions and reducing droplet coalescence. This trend corresponds to the partial denaturation of protein subunits such as β-conglycinin (7S), α, and α′, which unfold at temperatures between 78.6–90.8 °C [52]. The partially unfolded proteins possess increased surface activity, enhancing emulsion stability through better interfacial film formation [53]. Moreover, heat treatment has been shown to increase the flexibility of SPI molecules, facilitating their rearrangement at the oil–water interface and reducing interfacial tension [54].

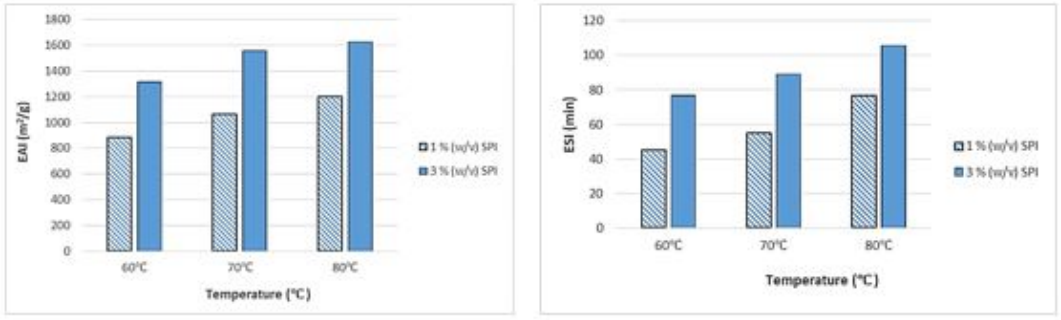

(a) (b)

Figure 3.5: Emulsifying properties of SPI-stabilized emulsions at different heating temperatures (a) EAI, (b) ESI

Creaming Behavior of Heat-Treated Emulsions

Creaming behavior was monitored over an 8-hour period and is illustrated in Figure 3.6. Emulsions containing 3% (w/v) SPI and subjected to thermal treatment at 80 °C exhibited the lowest creaming values, ranging from 8.1% to 9.4%, indicating enhanced physical stability. In contrast, emulsions formulated with 1% SPI showed higher creaming rates under the same thermal condition, with values ranging from 8.6% to 10.4%. Notably, at 60 °C, creaming in 1% SPI emulsions reached a peak of 16.7%,

whereas this value decreased significantly to 10.4% when treated at 80 °C ($p<0.05$). These findings clearly demonstrate that increasing both protein concentration and heat treatment temperature significantly reduces creaming, likely by enhancing interfacial coverage and viscosity, thereby minimizing droplet migration and phase separation. Heating causes protein unfolding, promoting stronger protein–oil interactions and facilitating the formation of a viscoelastic interfacial layer that limits droplet coalescence [41]. Thus, heat-induced modifications enhance protein adsorption and reduce phase separation in emulsions [52]. Dynamic light scattering and interfacial shear rheology analyses further confirm that heat-treated SPI forms more elastic and cohesive interfacial films, improving physical emulsion stability [55].

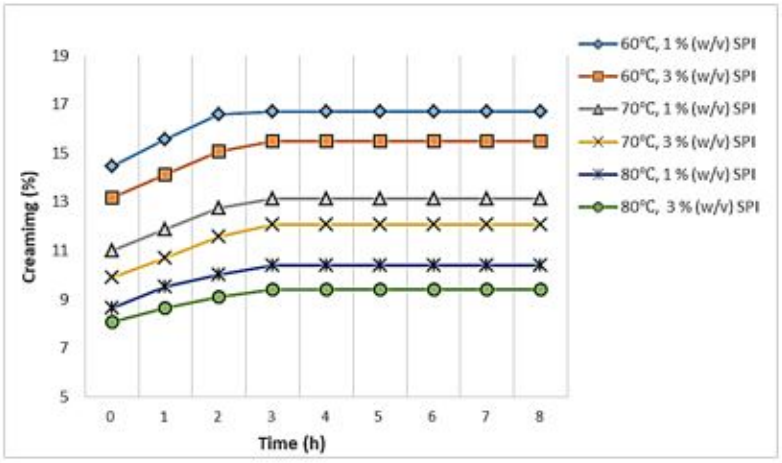

Figure 3.6: Creaming behavior of SPI-stabilized emulsions at different heating temperatures

Microstructure of Heat-Treated Emulsions

The microstructure of heat-treated emulsions is depicted in Figure 3.7, while corresponding droplet size values are presented in Table 3.1. Across all temperature conditions, emulsions formulated with 3% (w/v) SPI exhibited consistently smaller droplet sizes compared to those with 1% SPI, indicating more effective interfacial stabilization at higher protein concentrations. Specifically, at 60 °C, droplet sizes were 9.84 μm and 8.93 μm for 1% and 3% SPI, respectively. These values decreased significantly to 6.7 μm and 5.88 μm at 70 °C, and further to 4.54 μm and 4.17 μm at 80 °C ($p<0.05$). The observed reduction in droplet size with increasing temperature suggests that heat treatment facilitates partial unfolding of soy protein molecules, enhancing their ability to adsorb at the oil–water interface and form more stable, finely dispersed emulsions. Increased molecular flexibility and enhanced protein adsorption at the oil–water interface lead to the formation of more uniform and stable droplets [40, 47]. Additionally, the improved surface hydrophobicity of 7S globulin at higher temperatures contributes to better droplet interaction and emulsion stability [1]. Recent confocal laser scanning microscopy (CLSM) studies have visually confirmed that higher temperatures result in tighter, more homogeneous interfacial protein films around oil droplets, especially at higher SPI concentrations [56].

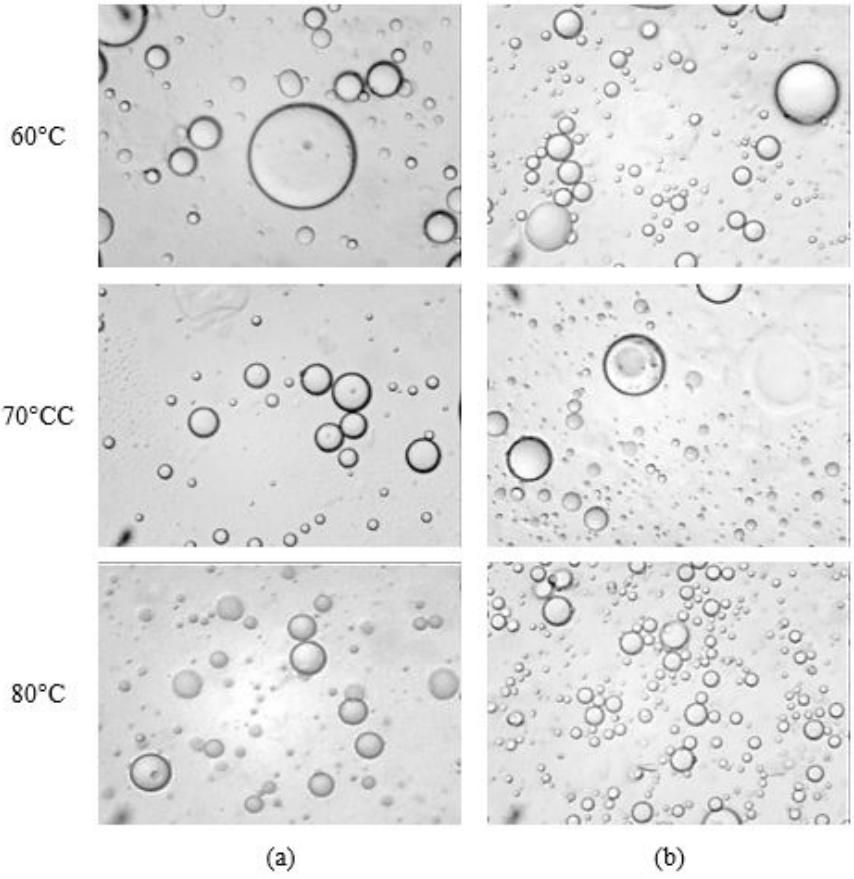

Figure 3.7: Microstructure of SPI-stabilized emulsions with varying protein concentrations at different heating temperatures: (a) 1% (w/v) SPI, (b) 3% (w/v) SPI

Viscosity of Heat-Treated Emulsions

The viscosity profiles of heat-treated emulsions are presented in Figure 3.8. For emulsions containing 1% (w/v) SPI, viscosity values slightly decreased from 1.6 cP at 60 °C to 1.4 cP at 80 °C. In contrast, emulsions with 3% SPI displayed substantially higher viscosity values of 3.0, 2.7, and 2.5 cP at 60, 70, and 80 °C, respectively. The observed decrease in viscosity with increasing temperature ($p<0.05$) may be attributed to enhanced protein unfolding, which facilitates better molecular dispersion and reduces entanglement within the continuous phase. These changes suggest that while higher protein concentration contributes to increased viscosity, thermal treatment may soften the structure by promoting a more uniform and less entangled protein network. This phenomenon has been previously linked to enhanced protein solubility and reduced intermolecular aggregation during thermal processing [57]. Such structural changes allow proteins to form more mobile, less viscous matrices without compromising stability. This temperature-induced viscosity reduction aligns with rheological modeling studies that report a shift from entangled network formation to more dispersed colloidal interactions at elevated temperatures [58].

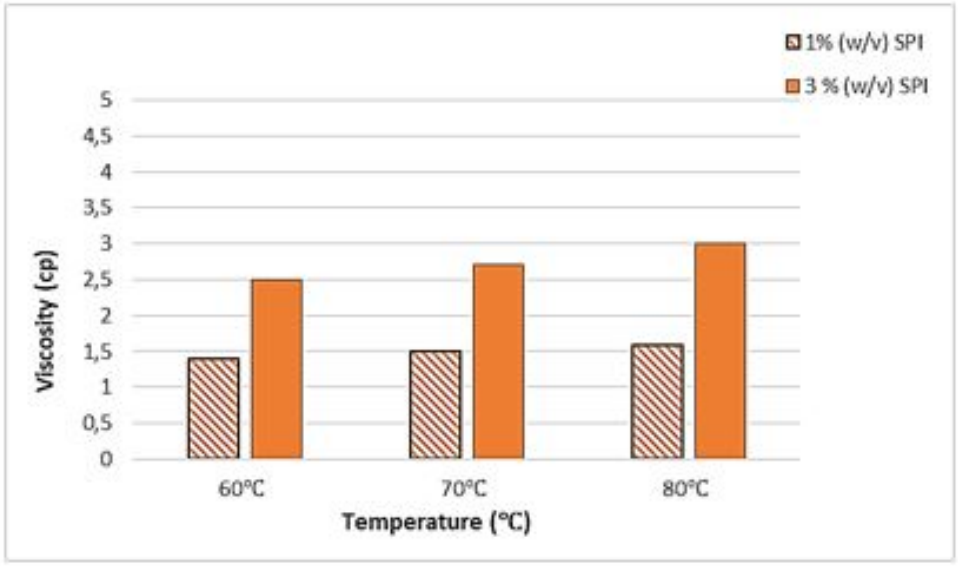

Figure 3.8: Viscosity of SPI-stabilized emulsions at different heating temperatures

Effect of pH on Emulsions

Emulsifying Activity and Stability Index of pH-Adjusted Emulsions

Figure 3.9a presents the EAI of SPI-stabilized emulsions at concentrations of 1% and 3% (w/v) across pH values of 5, 7, and 9. The lowest EAI values were recorded at pH 5, with 607.99 m^2/g for 1% SPI and 1229.80 m^2/g for 3% SPI. This reduction is attributed to decreased protein solubility near the isoelectric point (pI ≈ 4.8) of β-conglycinin, which limits protein migration and adsorption at the oil–water interface [59]. As the pH increased to 7 and 9, EAI values rose significantly ($p<0.05$), reaching 1192.95 m^2/g and 1975.97 m^2/g at pH 9 for 1% and 3% SPI, respectively. This increase is primarily due to enhanced protein solubility, elevated net surface charge, and intensified electrostatic repulsion among protein molecules, all of which contribute to improved dispersion, reduced aggregation, and more effective interfacial adsorption [51, 59]. Furthermore, the results consistently show that emulsions containing 3% SPI yielded higher EAI values at all pH levels, highlighting the importance of protein availability at the interface. Supporting evidence from recent studies using electrophoretic mobility and zeta potential analyses indicates that SPI exhibits increased ionization and net surface charge above pH 7, enhancing emulsifying activity through improved steric and electrostatic stabilization [60].

The emulsifying stability index (ESI) exhibited a trend similar to that of the EAI, as shown in Figure 3.9b. The highest stability was achieved at pH 9, with ESI values of 53.96 minutes for emulsions containing 1% SPI and 146.93 minutes for those with 3% SPI. Moderate stability was observed at pH 7, which approximates the native pH of soy proteins (≈7.2), while the lowest ESI values occurred at pH 5. This reduction near the isoelectric point reflects emulsion instability caused by increased protein aggregation and weakened interfacial film strength [33, 61]. These results further support the notion that pH conditions distant from the isoelectric point enhance protein functionality in emulsified systems by improving solubility and interfacial behavior. In particular, at alkaline pH, SPI exhibits stronger protein–protein interactions at the interface, contributing to the formation of thicker, more elastic interfacial films that effectively resist coalescence and creaming over time [62].

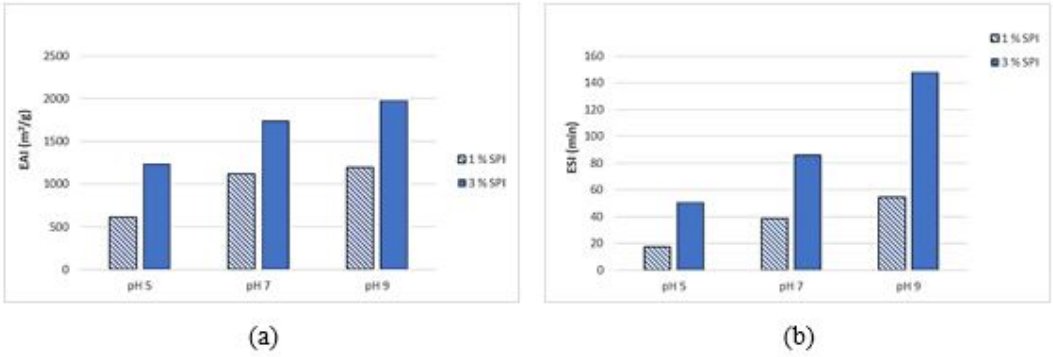

Figure 3.9: Emulsifying properties of SPI-stabilized emulsions at different pH values: (a) EAI, (b) ESI

Creaming Stability of pH-Adjusted Emulsions

The creaming behavior of SPI-stabilized emulsions across different pH levels is illustrated in Figure 3.10. The highest creaming rates were recorded at pH 5 for both 1% and 3% (w/v) SPI, reaffirming the reduced emulsion stability near the isoelectric point due to diminished protein solubility and weaker interfacial film formation. In contrast, emulsions at pH 9 demonstrated significantly lower creaming percentages ($p<0.05$) approximately 10% for 1% SPI and just 6% for 3% SPI, indicating enhanced physical stability under alkaline conditions. This improvement is likely attributed to increased electrostatic repulsion between droplets and greater interfacial adsorption of protein, both of which contribute to reduced coalescence and phase separation. These findings underscore the role of pH in modulating the structural and interfacial properties of protein-stabilized emulsions. Additionally, glycinin-rich fractions tend to dominate at basic pH and have been associated with stronger interfacial films and better droplet protection [63]. Overall, emulsions exhibited enhanced physical stability at higher pH levels, consistent with prior findings [52].Moreover, high-pH-treated SPI emulsions demonstrated improved oxidative stability and reduced droplet aggregation during storage, attributed to denser interfacial protein networks [65].

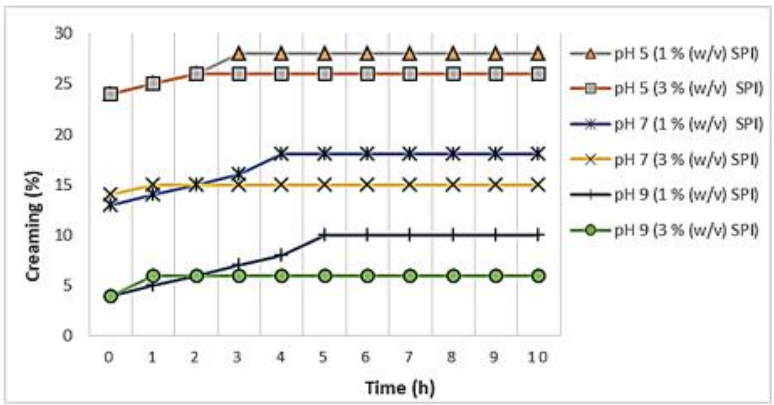

Figure 3.10: Creaming behavior of SPI-stabilized emulsions at different pH values

Microscopic Structure of pH-Adjusted Emulsions

Microscopic observations (Figure 3.11) and droplet size measurements (Table 3.1) provide clear evidence of the impact of pH on the microstructure of SPI-stabilized emulsions. At pH 9, droplet sizes were significantly smaller ($p<0.05$), 8.93 μm for 1% SPI and 6.17 μm for 3% SPI, and the emulsions exhibited a more uniform and finely dispersed structure, indicating enhanced emulsion formation and stability. In contrast, emulsions prepared at pH 5 displayed larger average droplet sizes, 10.91 μm and

9.78 μm for 1% and 3% SPI, respectively, along with irregular morphology and visible signs of coalescence and de-emulsification. These structural changes are attributed to reduced protein solubility near the isoelectric point, which leads to protein aggregation and the formation of weak interfacial films unable to prevent droplet fusion [33]. These results underscore the importance of pH in modulating interfacial behavior and maintaining structural integrity in protein-stabilized emulsions. The enhanced droplet uniformity at pH 9 is supported by recent studies, which highlight improved protein flexibility and charge repulsion under alkaline conditions as key drivers of structural stability [48, 53]. CLSM and SEM imaging studies confirmed that higher pH values lead to more continuous protein coatings around droplets, supporting their steric stabilization and preventing flocculation [66].

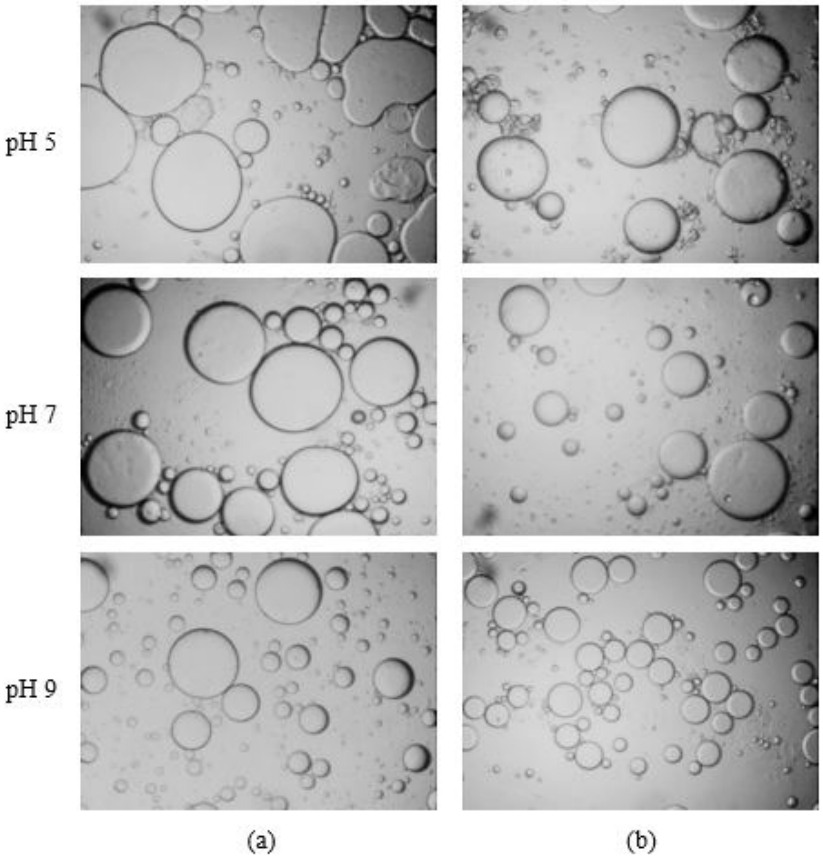

Figure 3.11: Microstructure of SPI-stabilized emulsions with varying protein concentrations at different pH values: (a) 1% (w/v) SPI, (b) 3% (w/v) SPI

Viscosity of pH-Adjusted Emulsions

Viscosity measurements of SPI-stabilized emulsions at varying pH levels are presented in Figure 3.12. For emulsions containing 1% (w/v) SPI, viscosity increased significantly from 0.36 cP at pH 5 to 0.57 cP at pH 9 ($p<0.05$). A similar trend was observed in 3% SPI emulsions, where viscosity rose from 0.76 cP to 1.23 cP as pH increased from 5 to 9. The lowest viscosity values at pH 5 are likely due to protein aggregation near the isoelectric point, which reduces water-binding capacity and promotes phase separation. In contrast, increasing the pH improved protein solubility and facilitated stronger intermolecular interactions, particularly in the higher protein concentration emulsions. This resulted in more structured continuous phases and enhanced viscosity, contributing to better emulsion stability under alkaline conditions. This is consistent with the behavior of soy proteins at alkaline pH, where protein molecules adopt expanded conformations, increasing hydrodynamic volume and resistance to flow [61]. Alkaline pH conditions also result in increased apparent viscosity and yield stress in SPI emulsions, as report-

ed in rheological modeling studies, due to enhanced electroviscous effects [63].

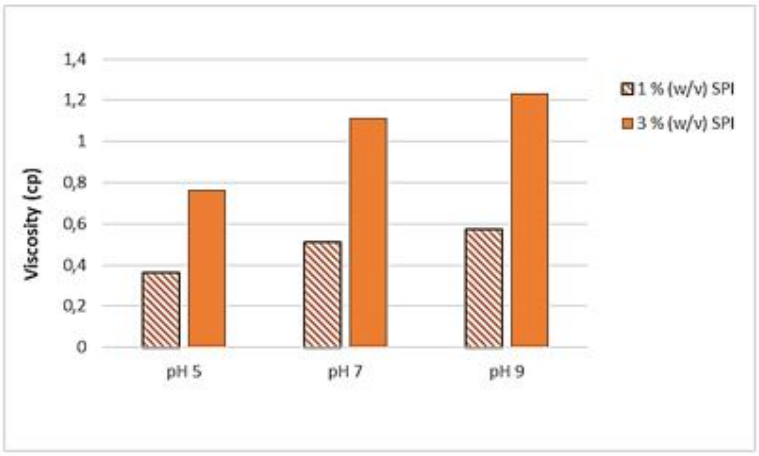

Figure 3.12: Viscosity of SPI-stabilized emulsions at different pH values

Properties of Gel-like Emulsions

Effects of Protein Concentration on Gel-like Emulsions

Gel formation was investigated by varying SPI concentrations (1%, 3%, 5%, 6%, 7%, 8%, and 10% w/v) under two oil levels (10% and 30% v/v). After 24 hours, only emulsions with 6% and 7% SPI concentrations formed distinct gel-like structures, suggesting the presence of a threshold for effective network formation. These results are consistent with previous findings by Campbell et al. [63], who identified a minimum SPI concentration necessary for physical gelation.

The gel-like emulsions formed at these concentrations were subsequently analyzed for water-holding capacity (WHC), fat-holding capacity (FHC), microstructure, and droplet size. Due to their semi-solid structure, conventional EAI and ESI measurements are not applicable, as oil droplets are entrapped within the protein matrix, limiting creaming. Higher protein levels increase interfacial coverage and protein–protein interactions, which enhance network stability and resistance to coalescence.

Previous studies indicated that SPI undergoes critical gelation above 5% w/v, particularly near neutral pH [51]. The findings of gelation at 6–7% SPI in present study support this threshold. Gel-like emulsions were developed using both cold-set and heat-set approaches. In the cold-set method, ultrasound-pretreated SPI was mixed with $CaSO_4$ as a coagulant; in the heat-set method, gels were further heated at 95 °C for 20 minutes. Zang et al. (2016) demonstrated that ultrasound pretreatment improves cold-set SPI gels by increasing WHC and solubility. $CaSO_4$ functions by neutralizing negative charges on protein surfaces at neutral pH, thereby promoting hydrophobic aggregation [64].

Recent studies show that combining ultrasound with salt-induced gelation enhances the viscoelastic behavior and molecular crosslinking of SPI gels, particularly at ≥6% concentrations [65]. Moreover, high-resolution rheometry indicates that SPI gels at 7–8% w/v exhibit a transition from viscoelastic liquid to solid-like behavior, marked by a significant increase in storage modulus (G′) [66].These gel systems are being explored for nutraceutical delivery due to their controlled release potential and high encapsulation efficiency for lipophilic compounds [54].

Water-Holding Capacity (WHC) of Gel-like Emulsions

Figures 3.13a and 3.13b depict the WHC of SPI-based gels formulated with 6% and 7% protein concentrations at oil levels of

10% (v/v) and 30% (v/v), respectively. WHC increased significantly ($p<0.05$) with both higher SPI concentration and elevated oil content. As shown in Figure 3.13a, the lowest WHC was observed in cold-set gels containing 6% SPI and 10% oil. In contrast, heat-set gels consistently exhibited higher WHC values across all formulations, which can be attributed to the development of more interconnected and compact protein networks during thermal treatment. These networks are more efficient in entrapping water, thereby enhancing gel hydration. An increase in oil concentration from 10% to 30% resulted in a statistically significant improvement in WHC for both cold- and heat-set systems ($p<0.05$), indicating a synergistic effect of lipid content and processing conditions on water retention. These findings are in agreement with previous research suggesting that heat treatment promotes protein swelling and cross-linking, leading to improved water-binding capacity [67]. Additional support comes from nuclear magnetic resonance (NMR) relaxation studies, which demonstrated enhanced water immobilization in thermally induced SPI gels [68].

A particularly noteworthy result was observed in Figure 3.13b, where the WHC of the 7% SPI with 30% oil formulation increased from 55% to 75% following heat treatment. This substantial enhancement is likely due to the increased availability of protein–water binding sites and the swelling of the gel matrix induced by thermal energy [63, 69] similarly reported that thermal processing enhances the hydrophobicity and WHC of SPI by inducing conformational rearrangements.

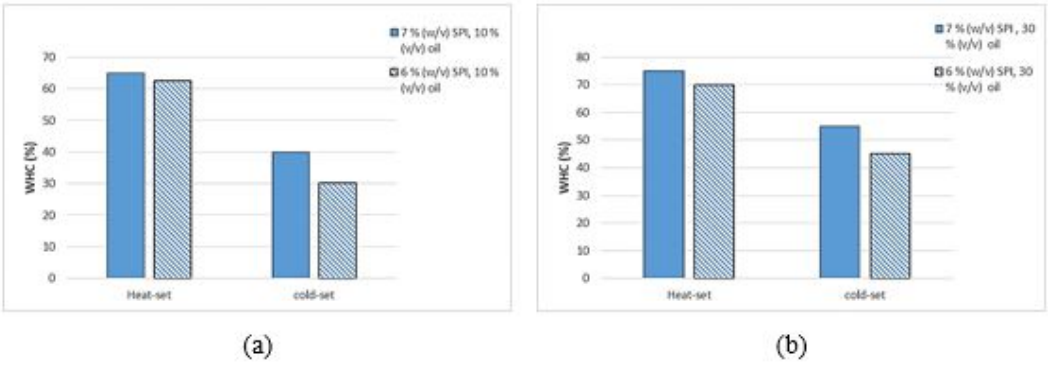

Figure 3.13: Water holding capacity of heat-set and cold-set gel-like emulsions at: (a) 10% oil concentration, (b) 30% oil concentration

Fat-Holding Capacity (FHC) of Gel-like Emulsions

Figures 3.14a and 3.14b illustrate the FHC of SPI-based gels prepared with varying protein concentrations (6% and 7% w/v) and oil contents (10% and 30% v/v). A statistically significant increase in FHC ($p<0.05$) was observed with both higher SPI concentration and increased oil levels. As depicted in Figure 3.14a, FHC at 10% oil increased from approximately 30% to 40% as SPI concentration rose from 6% to 7%. Cold-set gels with 6% SPI and 10% oil exhibited the lowest fat retention (~15%), whereas heat-set gels under the same formulation conditions retained twice as much (~30%).

An even more pronounced effect was observed at 30% oil content (Figure 3.14b), where FHC values were markedly higher. The highest FHC (approximately 60%) was recorded in heat-set gels prepared with 7% SPI and 30% oil, indicating the synergistic role of protein content, oil level, and thermal treatment in enhancing lipid retention. These results suggest that heat facilitates protein unfolding and reorganization, which in turn promotes stronger protein–lipid interactions and enables more efficient fat entrapment [33].

Supporting evidence from recent studies confirms that thermal gelation enhances the encapsulation of oil droplets within a continuous protein network, thereby improving lipid immobilization [35, 70] further reported that heat-induced dissociation of glycinin hexamers into subunits facilitates gel formation through interactions between 7S and 11S globulins. Additionally,

SPI-based heat-set gels exhibit superior oil barrier properties compared to cold-set counterparts, which may contribute to reduced oil migration in formulations such as low-fat meat analogues and plant-based spreads [70].

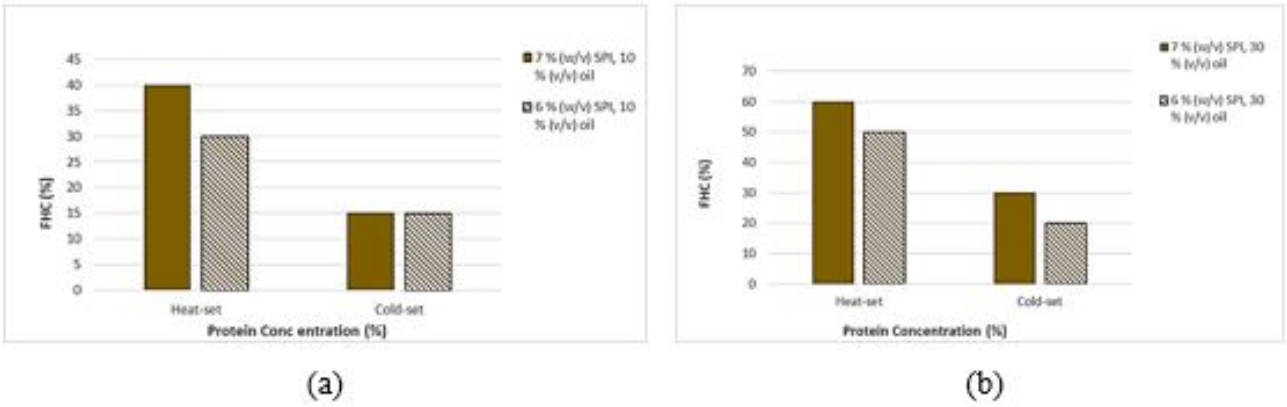

Figure 3.14: Fat holding capacity of SPI gel-like emulsions at: (a) 10% oil concentration, (b) 30% oil concentration

Microstructure of Gel-like Emulsions

Microscopic analysis results, presented in Table 3.2 and Figure 3.15, demonstrate a clear relationship between SPI concentration, oil content, and droplet size in gel-like emulsions. In cold-set gels formulated with 10% oil, increasing the SPI concentration from 6% to 7% (w/v) led to a significant reduction ($p<0.05$) in droplet size from 7.97 μm to 6.83 μm. A similar significant decreasing trend was observed when oil content increased from 10% to 30% at both protein levels ($p<0.05$), with droplet size decreasing to 7.11 μm and 5.98 μm for 6% and 7% SPI, respectively. These results suggest that both higher protein and oil levels contribute to more effective emulsification by reducing droplet coalescence. Furthermore, heat-set gels consistently exhibited smaller droplet sizes than their cold-set counterparts, indicating improved emulsification performance under thermal conditions. For instance, in 7% SPI gels with 30% oil, the droplet size decreased to 4.67 μm under heat-set conditions, compared to 5.98 μm in cold-set. This enhancement can be attributed to thermal treatment facilitating protein unfolding and improved interfacial adsorption, thereby stabilizing the emulsion more effectively and resulting in finer droplet distributions. The difference reflects the role of thermal denaturation in promoting protein–oil interactions and forming tighter gel networks [51]. Higher oil levels further reduced droplet size in heat-set systems due to enhanced hydrophobic interactions and better emulsification before gelation [52]. The smallest droplets (4.67 μm) were found in heat-set gels with 7% SPI and 30% oil, indicating optimal conditions for fine droplet stabilization and gel structure. Confocal imaging and droplet surface analysis show that the compact droplet network in heat-set gels is associated with higher G′ and reduced coalescence, which is ideal for targeted delivery systems [66].

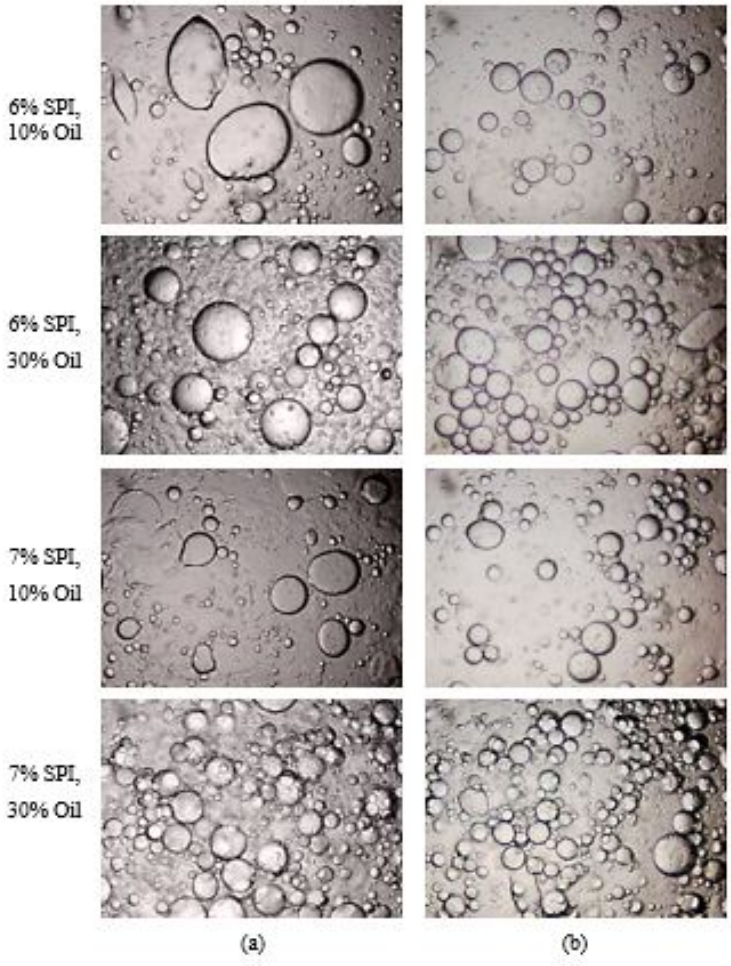

Figure 3.15: Microstructure (10× magnification) of SPI gel-like emulsions prepared by (a) cold-set and (b) heat-set methods at varying protein concentrations

Conclusion

This study comprehensively demonstrated that ultrasound treatment, thermal processing, and pH modulation have a significant impact on the physicochemical, emulsifying, and gel-forming properties of soy protein isolate (SPI) in emulsion-based systems. Ultrasound treatment, particularly at 15 amplitude, markedly enhanced emulsifying activity index (EAI), emulsifying stability index (ESI), viscosity, and creaming stability. These improvements were driven by ultrasound-induced partial unfolding and disaggregation of SPI molecules, which promoted enhanced interfacial adsorption, reduced droplet size, and a more homogeneous emulsion structure.

Heat treatment, especially at 80 °C, further amplified these effects. Thermal denaturation enhanced protein–oil interactions and facilitated the formation of more cohesive and compact interfacial films, resulting in finer droplet dispersion and superior microstructural uniformity. Similarly, pH played a critical role in protein functionality. Emulsions prepared under alkaline conditions (pH 9) exhibited significantly greater stability and emulsification efficiency compared to those near the isoelectric point (pH 5), due to improved protein solubility, increased surface charge, and stronger electrostatic repulsion. In all cases, higher protein concentration (3% vs. 1%) led to improved emulsifying properties, highlighting the importance of adequate protein availability for stabilizing oil–water interfaces.

These findings were further confirmed in gel-like emulsion systems. At SPI concentrations of 6% and 7%, both cold-set and heat-set methods successfully produced viscoelastic gel matrices. Heat-set gels demonstrated superior water-holding capacity (WHC) and fat-holding capacity (FHC), attributed to thermal aggregation, protein restructuring, and enhanced network formation. Microscopy and droplet size analysis supported these observations, revealing smaller, more uniformly distributed oil droplets in heat-set samples, particularly at higher SPI and oil concentrations.

From an application perspective, these optimized SPI-based emulsions and gel systems have promising potential in the formulation of functional foods. They may serve as fat replacers in low-fat meat products, structuring agents in sauces or dairy alternatives, and encapsulation platforms for sensitive bioactive compounds such as polyphenols, omega-3 fatty acids, or probiotics. The cold-set approach, in particular, offers advantages for incorporating heat-sensitive ingredients without compromising their bioactivity.

Looking forward, further research should investigate the synergistic effects of SPI with other plant proteins or polysaccharides, assess long-term stability under storage conditions, and evaluate sensory attributes relevant to consumer acceptance. Molecular-level analyses such as spectroscopy, proteomics, or molecular dynamics simulations, may also yield deeper insight into the structural mechanisms underlying the observed functionality.

Collectively, this study provides a robust foundation for the development of clean-label, plant-based emulsions and gel-like matrices with enhanced stability, nutritional functionality, and application versatility in modern food systems.

References

1. Nishinari K, Fang Y (2014) Soy proteins: A review on composition, aggregation and emulsification Food Hydrocolloids, 301–318.

2. Al-Bakkush A-AA (2008) Improvement of functional properties of soy protein (Master's thesis) Heriot-Watt University, School of Life Sciences.

3. Stone AK, Karalash A, Tyler RT, Warkentin TD, Nickerson MT (2015) Functional attributes of pea protein isolates prepared using different extraction methods and cultivars Food Research International, 31–38.

4. Zhao Q, Selomulya C, Xiong H (2020) Glycinin-rich soy protein fractions and their interfacial behavior in emulsion stabilization Food Chemistry, 125649.

5. Wu Q, Chen Y, Zhang L, Luo Y (2023) Effects of soybean protein peptides on gut microbiota and metabolic profiles in health management Journal of Functional Foods, 105370.

6. Granato D, Nunes DS, Barba FJ (2020) An integrated strategy for the development of functional foods and nutraceuticals Trends in Food Science & Technology, 106–120.

7. Milani JM, Golkar A (2019) Introductory chapter: Some new aspects of colloidal system in food In Some new aspects of colloidal systems in foods IntechOpen.

8. Li J, Liu X, Li X, Wang Z (2022) Microencapsulation of phytochemicals using soy protein-based matrices: A comprehensive review Trends in Food Science & Technology, 12–23.

9. Damodaran S, Paraf A (Eds.) (1997) Food proteins and their applications Marcel Dekker.

10. Schmidt US, Gruner J, Schuchmann HP (2022) Techno-functional properties of alternative proteins: Challenges and solutions Current Opinion in Food Science, 100849.

11. Day L (2013) Proteins from land plants—Potential resources for human nutrition and food security Trends in Food Science & Technology, 25–42.

12. Mession JL, Sok N, Assifaoui A, Saurel R (2022) New insights in plant protein functionality Trends in Food Science & Technology, 201–216.

13. Fukushima D (2004) Soy proteins In RYYada (Ed.), Proteins in food processing (pp. 262–288) Woodhead Publishing.

14. Hu H, Li-Chan ECY, Wan L, Tian M, Pan S (2013) The effect of high-intensity ultrasonic pretreatment on the properties of soybean protein isolate gel induced by calcium sulfate Food Hydrocolloids, 303–311.

15. Renkema JMS (2001) Formation, structure and rheological properties of soy protein gels [Doctoral dissertation, Wageningen University] Wageningen University Repository.

16. Utsumi S, Matsumura Y, Mori T (1997) Structure–function relationships of soy proteins In S Damodaran, A Paraf (Eds.) Food proteins and their applications (pp. 257–291) Marcel Dekker.

17. Chen F, Zhang H, Tang CH, Li B (2021) Effects of ultrasound on the physicochemical and gelation properties of soy protein isolate–pectin complexes Food Hydrocolloids, 106467.

18. Ma Y, Wang J, Zhang R, Tang C (2023) Structural and dynamic insights into gelation of soy protein isolate via low-field NMR and CLSM LWT - Food Science and Technology, 114283.

19. Dickinson E (2020) Emulsion gels: The structuring of soft solids with protein-stabilized oil droplets Food Hydrocolloids, 106089.

20. Liu F, Tang C (2014) Emulsifying properties of soy protein nanoparticles: Influence of protein concentration and/or emulsification process Journal of Agricultural and Food Chemistry, 2644–2654.

21. McClements DJ (2021) Development of next-generation functional food systems using structural design principles Annual Review of Food Science and Technology, 1–27.

22. Tang C, Liu F (2013) Emulsion gels as delivery systems for bioactive food components: Influence of gelation conditions and structure–function relationship Food Hydrocolloids, 191–199.

23. Gao Y, Lu Y, Wang Y, Xu X (2021) Polysaccharide–soy protein complexes for improved stability of functional emulsions: A review Carbohydrate Polymers, 118183.

24. Sun Q, Hu X, Liu J, Tang C (2024) Interfacial design of plant protein–dietary fiber emulsions for improved oxidative and physical stability Food Chemistry, 137074.

25. Jambrak AR, Lelas V, Mason TJ, Kresic G, Badanjak M (2009) Physical properties of ultrasound treated soy proteins Journal of Food Engineering, 386–393.

26. O'Sullivan J, Park M, Beevers J (2016) The effect of ultrasound upon the physicochemical and emulsifying properties of

wheat and soy protein isolates Journal of Cereal Science, 77–84.

27. Gülseren İ, Coupland JN (2012) Structural changes in soy protein isolate upon ultrasound treatment Food Research International, 82–89.

28. Zang P, Hu T, Feng S, Xu Q, Zheng T, Zhou M, Hu H (2016) Effect of high-intensity ultrasound on transglutaminase-catalyzed soy protein isolates cold set gel Ultrasonics Sonochemistry, 380–387.

29. Zhao Y, Wang J, Zhang R (2021) Synergistic effects of pulsed electric field and ultrasound on plant protein emulsions Ultrasonics Sonochemistry, 105423.

30. Liang H, Ma L, Zhao G (2023) Enhancing functional properties of soy protein by combined high-intensity ultrasound and ohmic heating Innovative Food Science & Emerging Technologies, 103119.

31. Koubaa M, Barba FJ, Roohinejad S, Fabiano-Tixier AS, Vorobiev E (2015) Current and new insights in the sustainable and green recovery of nutritionally valuable compounds from Stevia rebaudiana Bertoni Journal of Agricultural and Food Chemistry, 6835–6846.

32. Wang X, Zhang Y, Chen Y, He Y (2025) Predictive modeling and optimization of soy protein gelation using advanced rheokinetic parameters Journal of Food Engineering, 111611.

33. Gu X, Campbell LJ, Euston SR (2009) Effect of different oils on the properties of soy protein isolate emulsions and gels Food Research International, 925–932.

34. Li F, Kong X, Zhang C, Hua Y (2012) Gelation behavior and rheological properties of acid-induced soy protein-stabilized emulsion gels Food Hydrocolloids, 347–355.

35. Pietrasik Z, Janz JAM (2020) Gelation behavior of soy proteins: Impact of heating and lipid content Food Structure, 100145.

36. Helmick H, Ettestad S, Kokini JL (2023) Estimation of cold denaturation temperature and its utilization in predicting protein stability as an aid in functionalizing pea protein isolate through cold denaturation Innovative Food Science and Emerging Technologies, 103479.

37. Wang X, Tang CH, Li BS, Yang XQ, Li L, Ma CY (2008) Effect of high pressure treatment on some physicochemical and functional properties of soy protein isolate Food Hydrocolloids, 560–567.

38. Yang M, Liu F, Tang CH (2013) Properties and microstructure of transglutaminase-set soy protein-stabilized emulsion gels Food Research International, 409–418

39. Erçelebi EA, Kara Ş, İbanoğlu E (2011) Stability of bitter orange juice-olive oil salad dressings with polysaccharides Journal of Food Science and Engineering, 297–302.

40. Aryee A, Agyei D, Udenigwe CC (2018) Proteins in food processing (2nd ed.) Woodhead Publishing.

41. Dickinson E (1998) Structure, stability and rheology of flocculated emulsions Current Opinion in Colloid & Interface Science, 633–638.

42. McClements DJ (1995) Advances in the application of ultrasound in food analysis and processing Trends in Food Science &

Technology, 293–299.

43. Chemat F, Rombaut N, Sicaire AG, Meullemiestre A, Fabiano-Tixier AS, Abert-Vian M (2017) Ultrasound-assisted extraction of food and natural products: Mechanisms, techniques, combinations, protocols and applications—A review Ultrasonics Sonochemistry, 540–560.

44. Tavano OL, Neves VA, Rosa CDS (2021) Effects of high-intensity ultrasound on structure and functional properties of proteins: A review Trends in Food Science & Technology, 593–603.

45. Chen Y, Ma K, Wang D (2022) Recent advances in improving water-holding and fat-binding properties of plant protein gels Food Hydrocolloids, 107369.

46. Li M, Tang C, Zhang Y (2023) Fluorescence spectroscopy reveals interfacial behavior of sonicated soy protein emulsions Food Hydrocolloids, 108514.

47. Zhu Z, Zhou T, Wang H, Yang X, Zhao Q (2022) Effect of ultrasound on protein structural modification and emulsion stability: A systematic overview Food Chemistry, 131721.

48. Wang H, Liu G, Chen F, Zhao X (2021) Evaluation of emulsion stability by Turbiscan: Application to ultrasound-modified soy proteins Colloids and Surfaces A: Physicochemical and Engineering Aspects, 127171.

49. Jambrak AR (2017) Physical properties of sonicated products: A new era for novel ingredients In D Bermudez-Aguirre (Ed.), Ultrasound: Advances in food processing and preservation (pp. 73–94) Academic Press.

50. Ye A, Cui J, Dalgleish D, Singh H (2018) Role of ultrasound in structuring of food emulsions Advances in Colloid and Interface Science, 356–366.

51. Zhou L, Wu Y, Zhang L (2023) Interfacial protein distribution and microstructure of HIU-treated soy protein emulsions: A CLSM and SEM study Food Structure, 100330.

52. Liu Y, Zhang Q, Wang R, Liu X (2024) Rheological characteristics and modeling of ultrasound-modified SPI emulsions Journal of Texture Studies, e12978.

53. Liu F, Ma C, McClements DJ, Guo M (2022) Heat treatment of plant proteins: Physicochemical, structural, and functional modifications Comprehensive Reviews in Food Science and Food Safety, 81–102.

54. Wang H, Feng J, Xu Q (2023) Heat-induced structural transitions of soy protein isolate and their impact on emulsification: Insights from FTIR and CD spectroscopy Journal of Agricultural and Food Chemistry, 725–733.

55. Nishinari K, Fang Y, Nagano T, Guo S, Wang R (2018) Soy as a food ingredient In RYYada (Ed.) Proteins in food processing (2nd ed., pp. 235–270) Woodhead Publishing.

56. Tang CH (2020) Emulsifying properties of plant proteins: Recent developments and future perspectives Trends in Food Science & Technology, 113–126.

57. Chen M, Zhang Q, Li Y (2021) Structural and interfacial modifications of soy protein isolate under thermal treatment Food Chemistry, 129164.

58. Sun T, Zhao X, Wu Y (2022) Soy protein-based hydrogel systems for bioactive compound delivery: A review of formation mechanisms and applications Trends in Food Science & Technology, 270–281.

59. Chen W, Li X, Al-Hajj NM, Dey KC, Raqib SMMR (2014) Emulsification properties of soybean protein: A review Nusantara Bioscience, 196–202.

60. Jiang L, Wang X, Li R, Zhang T (2020) Visualization of heat-induced SPI-stabilized emulsions using CLSM: Effects of protein concentration and temperature Food Structure, 100149.

61. Li M, Sun Q, Zhang H (2020) Heat-induced gelation properties of SPI: Structural evolution and functional performance Journal of Food Engineering, 109930.

62. Zhou L, Wen J, Zhao X (2024) Rheological response of SPI emulsions at varied pH: Modeling the electroviscous effect Food Hydrocolloids, 108768.

63. Campbell LJ, Gu X, Dewar SJ, Euston SR (2009) Effect of heat treatment and glucono-δ-lactone-induced acidification on the characteristics of soy protein isolate Food Hydrocolloids, 344–351.Zheng X, Ma C, Liu G (2024) Thermal and rheological behavior of soy protein-based emulsions: A model-based approach Food Hydrocolloids, 108647.

64. Maltais A, Remondetto GE, Subirade M (2009) Soy protein cold-set hydrogels as controlled delivery devices for nutraceutical compounds Food Hydrocolloids, 1647–1653.

65. 3.Yang Y, Liu Q, Zhang B (2021) Synergistic enhancement of cold-set SPI gelation via ultrasound and calcium ion induction Ultrasonics Sonochemistry, 105419.

66. Kang Z, Wang J, Liu Y (2023) Modulation of gelation behavior of soy protein isolate by protein concentration and ultrasound: Rheological and structural insights Food Hydrocolloids, 108870.

67. Chen Z, Li Y, Zhang H, Wu J (2022) Structural modifications of soy protein isolate by high-intensity ultrasound: A proteomic and functional analysis Ultrasonics Sonochemistry, 105978.

68. 13.Zhou Y, Wang H, He Q (2023) Molecular water distribution in SPI gels: Insights from low-field NMR and water-binding capacity correlation Food Chemistry, 135025.

69. Farooq Z, Boye JI (2011) Novel food and industrial application of pulse flours and fractions In BKTiwari, B McKenna, A Gowen (Eds.), Pulse foods: Processing, quality and nutraceutical applications (pp. 283–299) Academic Press.

70. Utsumi S, Damodaran S, Kinsella JE (1984) Heat-induced interactions between soybean proteins: Preferential association of 11S basic subunits and beta subunits of 7S Journal of Agricultural and Food Chemistry, 1406–1412

71. Wang W, Zhang H, Xiong YL (2021) Role of calcium salts in plant protein gelation: Interactions and structural mechanisms Food Chemistry, 129875

72. Liu F, Ma C, McClements DJ, Guo M (2020) Effects of pH and ionic strength on the emulsifying properties of plant proteins: A review Trends in Food Science & Technology, 120–132.

73. Wang Q, Chen J, Feng J (2022) Zeta potential and protein solubility as indicators of emulsion stability in pH-shifted soy protein systems Colloids and Surfaces A: Physicochemical and Engineering Aspects, 128542.

74. Malekzadeh A, Hosseini SM, Yousefi G (2021) pH-dependent physicochemical properties of protein-stabilized emulsions: A review Journal of Molecular Liquids, 117391.

75. Zhang R, Liu P, Tang C (2023) Interfacial adsorption behavior and emulsifying performance of soy protein at alkaline pH: A film elasticity perspective Journal of Food Engineering, 111594.

76. Zhao X, Zhu J, Wang S (2020) Soy protein hydrolysate as a functional and nutritional ingredient: A review Food Research International, 109519.

77. Liu Z, Wang T, Cheng Y (2023) Oxidative and physical stability of pH-modified soy protein emulsions during storage Food Hydrocolloids, 108029.

78. Huang X, Ma X, Li Y (2021) Structural characterization and interfacial behavior of soy protein emulsions at different pH levels: A confocal and electron microscopy study Food Structure, 100204.

79. Li Y, Lv Y, Tang CH (2020) Heat-induced structural changes of plant proteins and their relationship with emulsion stability Food Hydrocolloids, 105581.

80. Chemat F, Huma ZE, Khan MK (2011) Application of ultrasound in food technology: Processing, preservation, and extraction Ultrasonics Sonochemistry, 813–835.

81. Phillips GO, Williams PA (2011) Introduction to food proteins In GO Phillips, PA Williams (Eds.) Handbook of food proteins (pp. 1–12) Woodhead Publishing.

82. Zhao Y, Li S, Zhou W (2022) Improving heat stability of soy protein emulsions via interfacial film engineering Food Hydrocolloids, 107637.

83. Pearce KN, Kinsella JE (1978) Emulsifying properties of proteins: Evaluation of a turbidimetric technique Journal of Agricultural and Food Chemistry, 716–723.